Geocarto International, 2014
Vol. 29, No. 4, 383–399, http://dx.doi.org/10.1080/10106049.2013.776643

Applying broadband spectra to assess biological control of saltcedar in west Texas

Reginald S. Fletcher*

USDA-ARS-Crop Production Systems Research Unit, Stoneville, MS 38766, USA

(*Received 20 August 2012; final version received 12 February 2013*)

Broadband field spectra were assessed to discriminate invasive saltcedar (*Tamarix* spp.) trees exhibiting feeding damage caused by the saltcedar leaf beetle (*Diorhadba* spp.) from other land cover types. Data were collected at two study sites near Presidio, Texas in 2010 and 2011. Spectral bands evaluated were coastal blue (400–450 nm), blue (450–510 nm), green (510–580 nm), yellow (585–625 nm), red (630–690 nm), red-edge (705–745 nm), and near-infrared (770–895, 860–1040 nm). Data were evaluated with analysis of variance and Scheffe's multiple comparison test ($\alpha = 0.05$). The red band generally separated severely damaged saltcedar trees from other land cover features. Near-infrared bands separated defoliated saltcedar trees. Broadband spectra has potential for distinguishing saltcedar trees exhibiting feeding damage caused by the saltcedar leaf beetle from other associated features, thus supporting future explorations of airborne and satellite-borne multispectral systems to monitor biological control of saltcedar within complex landscapes.

Keywords: saltcedar; saltcedar leaf beetle; multispectral; feeding damage; *Diorhadba* spp.

1. Introduction

Tamarix spp. commonly called saltcedar was introduced into the United States (US) over 100 years ago. Saltcedars are dense shrub or tree like plants native to Eurasia. Approximately, ten species are present in the US (United States Department of Agriculture [USDA] 2005). The plants have been used for ornamentals, windbreaks, and stream channel stabilisation. Several species are listed on invasive plant lists (DiTomaso 1998). *Tamarix ramosissima*, *T. chinensis*, and its hybrid cause the most damage in riparian areas of the US. *T. ramosissima* × *T. chinensis* hybrid is the most widespread in the US (Gaskin & Schaal 2003).

Several factors contribute to the invasiveness of saltcedars. The plants are prolific producers of seeds and develop them throughout the growing season, compared with other trees such as cottonwood (*Populus* spp.) and willows (*Salix* spp.) that produce seeds only in the spring. This seed production results in more opportunities for the plant to establish itself in riparian areas (DeLoach et al. 2003; Zouhar 2003; USDA 2005). Saltcedars are classified as phreatophytic and facultative halophytic plants. With their elaborate root systems, saltcedars outcompete native vegetation for water and nutrients, thus outgrowing surrounding vegetation. Its growth is not impeded by salty water

*Email: reginald.fletcher@ars.usda.gov

because the plant absorbs the salt via cell membranes (DiTomaso 1998). The leaves excrete the salts; salt-filled leaves dropped to the ground, alleviating the toxic affect of salty water. Salt excretion from leaves and leaf drop increases surface soil salt content. Only plants that are extremely salt-tolerant are able to grow in areas beneath saltcedar trees (Zouhar 2003). Mature plants are able to withstand drought for extended periods of time and can tolerate flooding for approximately 70 days (BASF 2005). Saltcedars are not a preferred food source by animals, further increasing their ability to establish in riparian areas (USDA 2005).

Detailed information pertaining to saltcedar impacts in an infested area has been published in the literature (Blackburn et al. 1982; Brotherson & Field 1987; DeLoach 1991; DiTomaso 1998; Tracy & DeLoach 1999; DeLoach et al. 2000, 2003, 2006; Dudley et al. 2000; Bailey et al. 2001; USDA 2005); thus, a brief description is provided here. Negative impacts of its invasions include excessive water use by the plant; increases in sedimentation within the water system and narrowing of the water channel (causes flooding); decrease in water flow; reduction in abundance and diversity of plants and animals occurring in riparian habitats; increases in the incidence of fire from accumulation of heavy litter fall, saltcedar leaves, and dead wood material; increases in soil salinity; and decline in recreational usage of infested areas for camping, hunting and fishing, boating, bird watching, and wildlife photography. Saltcedar invasions also have an adverse influence on certain listed threatened and endangered species.

Examples of saltcedar effects on threatened and endangered species are as follows. Along the Mojave River in southern California, USA, the protected western pond turtle (*Clemmys marmorata*) and the endangered desert salamander (*Batrachoseps aridus*) habitats have been negatively impacted because of water removal and modification of channel geomorphology by saltcedars (Lovich et al. 1994; Lovich & DeGouvenain 1998). DeLoach et al. (2000) indicated that 34 species of fish are located in saltcedar infested areas within the US, leading to degradation of their habitats because of reduced water levels, modified channel morphology, silted backwaters, altered water temperature, and reduced and modified food resources. Endangered fish affected by saltcedars include the Rio Grande silvery minnow (*Hybognathus amarus*), the Colorado squawfish (*Pytocheilus lucius*), and the desert pupfish (*Cyprinodon macularis*) (DeLoach et al. 2000). Saltcedar invasions have also caused a reduction in the population of the threatened Pecos sunflower (*Helianthus paradoxus*) (DeLoach et al. 2000). Removal of saltcedars resulted in an increase in the sunflower populations (US Fish and Wildlife Service 1998; Tracy & DeLoach 1999).

Evaluating and implementing strategies to control this invasive plant has become a major priority of local, state, and federal government agencies. Approaches involving mechanical removal, fire, and herbicidal treatments are costly and are not effective for killing saltcedar and reducing its spread to other areas (DeLoach et al. 2006). Additionally, tactics involving herbicides have had a negative impact on the environment (DeLoach et al. 2000; USDA 2005). Biological control of saltcedar with the *Diorhabda* spp. (i.e. saltcedar leaf beetle) is gaining popularity because it does not impact soil and water quality and has shown good potential for the control of saltcedar (Lewis et al. 2003; DeLoach & Carruthers 2004; DeLoach et al. 2006). Furthermore, it is relatively inexpensive to continue the programme once the beetles have established themselves (Knutson et al. 2011).

Biological control involves the saltcedar leaf beetles and larvae feeding on the foliage of saltcedar plants, leading to a reduction in chlorophyll and photosynthesis. That action decreases starches and sugars produced by the plant (Knutson et al. 2009).

Defoliation by beetles and larvae is a continuous process starting in late spring and ending in early fall (Knutson et al. 2011). After defoliation by beetle and larvae, the plant does refoliate (Knutson et al. 2011). It expends energy and uses reserves to complete this process, weakening the tree and eventually resulting in tree death over time (Knutson et al. 2011).

In Texas, the first release of the saltcedar leaf beetle to control saltcedar invasions began in 2004 (Knutson et al. 2009). Periodically, releases have occurred at various regions throughout the state. Natural resource managers, federal, state, and local government officials, and scientists need effective means for monitoring biological control of saltcedar in Texas. This information is pertinent for tracking beetle movement and for evaluating effectiveness of the biological control programme.

Remote sensing instruments including ground, aerial, and satellite systems have shown promise as tools for monitoring biological control of saltcedar. Field reflectance in the green region (centred wavelength 550 nm; band range 546–555 nm) of the light spectrum was useful for separating healthy saltcedar plants from those with moderate to severe feeding damage (Everitt et al. 2007). Also, Everitt et al. (2007) employed airborne conventional colour photography to derive a map showing healthy and stressed saltcedar trees exhibiting feeding damage caused by the saltcedar leaf beetle. Dennison et al. (2009) derived vegetation indices with Advanced Spaceborne Thermal Emission and Reflection Radiometer (ASTER) and Moderate Resolution Imaging Spectroradiometer satellite data and used the indices to monitor beetle defoliation of saltcedar trees at a study site in Utah for three years. In a qualitative assessment of hyperspectral imagery obtained with the Compact Airborne Spectrographic Imager, Anderson et al. (2005) distinguished healthy saltcedar trees from saltcedar trees damaged by beetle and larvae feeding.

In reality, other vegetation types, soil, and even human made features are part of the landscape in areas invaded by saltcedars. Using normalised difference vegetation index imagery derived with ASTER imagery, Dennison et al. (2009) indicated that cultivated vegetation types such as alfalfa, chemically treated saltcedar plants, disturbances to other vegetation types, and mechanical removal of saltcedar trees may have similar image responses to saltcedar trees defoliated by *Diorhabda* spp., leading to those features being falsely identified as *Diorhabda* defoliated saltcedar trees. More information is needed on application of remote sensing as a tool to separate saltcedar trees displaying stress from saltcedar beetle and larvae feeding from other land cover features. This study was conducted to evaluate broadband spectra within visible, red-edge, and near-infrared wavelengths to discriminate saltcedar trees exhibiting feeding damage caused by the saltcedar leaf beetle from other land cover types.

2. Materials and methods

2.1. Study sites

Two study sites in the Chihuahuan Desert were evaluated for this study. Site 1 (29° 31.163 N, 104° 16.880′ W) consisted of 4.5 ha and was located 9 km southeast of Presidio, TX, on Alamito Creek Ranch (Figure 1). Saltcedar (*T. chinensis* × *T. ramosissima* complex), catclaw (*Acacia* spp.), cheeseweed (*Hymenoclea monogyra)*, western honey mesquite (*Prosopis glandulosa* var. *torreyana*), and Bermuda grass (*Cyndon* spp.) were the dominant trees and shrub species observed within the study site. Non-vegetative features included bare soil (Riverwash and Pantera Soils, 0–2% slopes, frequently flooded), blacktop-road, and gravel. Saltcedar beetle (*Diorhabda sublineata*)

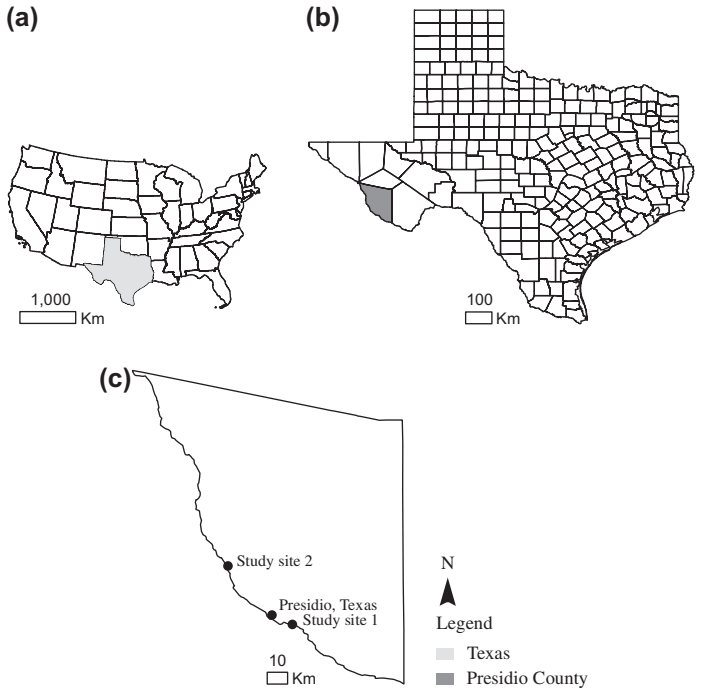

Figure 1. (a) Map of the contiguous US with the state of Texas highlighted in grey, (b) close-up of Texas counties and the location of Presidio County, and (c) close-up of Presidio County and location of study sites in reference to Presidio, Texas.

release occurred during 2009 (personal communications, Jack DeLoach and James Tracey). Site 2 (29 46.501 N, 104° 33.979 W) consisted of a 3.3 ha area and was 30 km northwest of Presidio, TX. Prevailing vegetation included saltcedar and western honey mesquite. Other features observed were bare soil (Riverwash and Pantera Soils, 0–2% slopes, frequently flooded), blacktop-road, plant litter, and gravel. This study area was not selected as a beetle release site; nevertheless, it was between two sites in which *D. sublineata* was released. In west Texas, Sul Russ University has an on-going programme in which field surveys are conducted to confirm the presence of saltcedar leaf beetles and larvae (counts of beetles and larvae) at release sites, to determine damage caused by the beetles and larvae feeding (drive-by-surveys), and to provide general information pertaining to beetle movement (Ritzi & Hilscher 2010, 2011). This programme has been established since 2008. Based on their surveys, the damage to saltcedar trees were caused by the saltcedar leaf beetle and larvae feeding. For both study sites, average annual maximum and minimum temperatures are 30 and 12 °C, respectively. Typical rainfall is 27.4 cm per year.

2.2. Field spectra collection

Spectral data were collected at site 1 on 24 August 2010, and 28 October 2010, and at site 2 on 9 September 2010, and 21 July 2011. During beetle and larvae feeding, saltcedar tree canopies will turn from green (healthy) to a mixture of green, yellow-green, and orange brown foliage (immediate feeding damage), and finally to orange foliage (severe feeding damage; Everitt et al. 2007, Figure 2). Totally defoliated trees appear

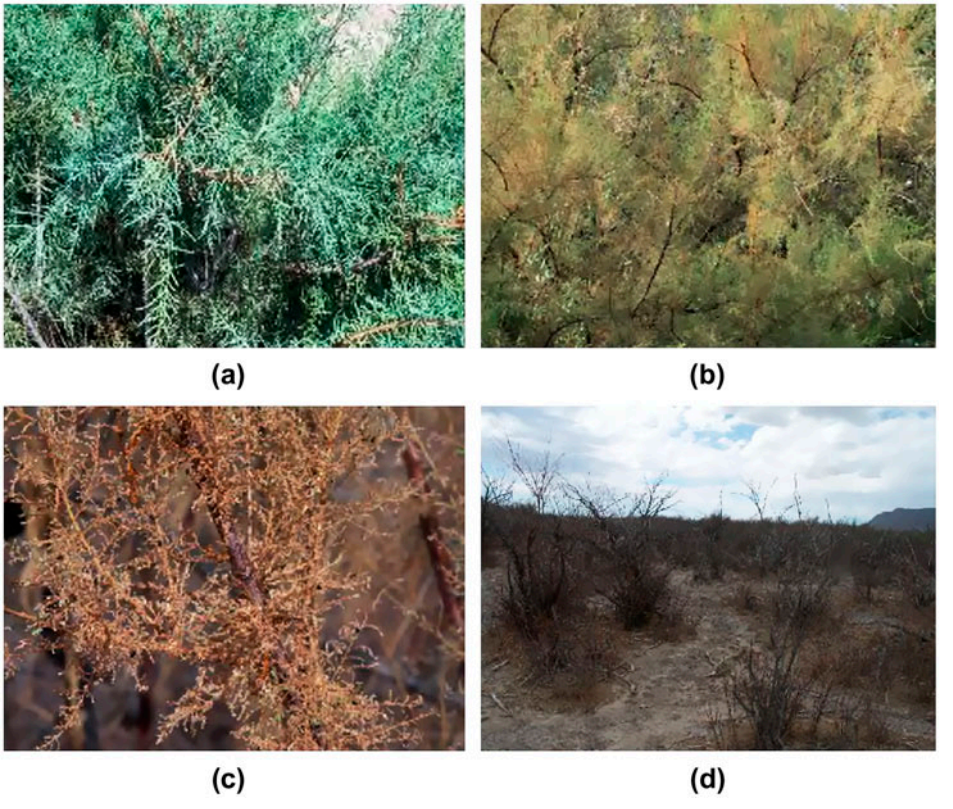

Figure 2. Ground level photos of saltcedar foliar symptoms associated with beetle and larvae feeding: (a) healthy plant-green, (b) intermediate damage-mixtures of green, yellow-green, and orange foliage, (c) severe damage-orange foliage, and (d) total defoliation of saltcedar trees.

dark grey (Figure 2). At the time of data collection, saltcedar canopies appeared in one or more of the colour stages and were labelled accordingly – healthy, intermediate feeding damage, severe feeding damage, and totally defoliated (Everitt et al. 2007).

An Analytical Spectral Devices FieldSpec3 full range-spectrometer (Analytical Spectral Devices, Inc., Boulder, CO) was used to collect the spectral data. It has a spectral range of 350–2500 nm. Spectral resolution is 3 nm at 700 and 10 nm at 1300/2500 nm. The software employed to operate the instrument resamples the data to 1 nm spectral intervals. The spectral data ranges from a value of 0–1, equivalent to 0–100% reflectance, respectively. The fibre optic attached to the spectrometer has a 25° viewing angle. During field surveys, it was attached to a pistol grip and was held 1 m above the feature of interest, resulting in a field of view 0.696 m^2. Each spectrum was an average of ten spectra. The instrument was calibrated at ten minute intervals with a spectralon white reference panel. Spectral data were collected under sunny conditions ±2 h of solar noon and were collected at random locations accessible by foot.

2.3. Post processing of field spectral data

To make sure that no erroneous data were collected, post processing consisted of viewing the spectra with the ViewSpec Pro (version 5.6.10, Analytical Spectral Devices,

Inc., Boulder, CO) software. Also, it was used to group and to export the data for further processing into Microsoft Office Excel (version 2007, Redmond, Washington). Broadband spectra corresponding to the coastal blue (400–450 nm), blue (450–510 nm), green (510–580 nm), yellow (585–625 nm), red (630–690 nm), red-edge (705–745 nm), near-infrared 1 (770–895 nm), and near-infrared 2 (860–1040 nm) bands of WorldView 2 satellite were tabulated with the band equivalent reflectance (BER) equation.

$$R_x = \sum_{i=\lambda\min}^{\lambda\max} ri\,pi \Big/ \sum_{i=\lambda\min}^{\lambda\max} ri \tag{1}$$

R_x represents BER for band x, λ min and λ max represent minimum and maximum reflectance, respectively, of band x's filter function, ri equals relative response for band x at wavelength i, and pi equals relative reflectance measured by the spectrometer at wavelength i (Trigg & Flasse 2000). Relative response values were obtained from Digital Globe, Inc. These bands were chosen because the blue, green, red, and near-infrared (1) bands are similar to those found on other broadband sensors. The additional bands are also relevant to vegetation applications.

2.4. Statistical analysis

The number of samples analysed for each land cover feature is shown in Table 1. Summary statistics (mean and standard errors), unbalanced one-way analysis of variance (ANOVA; $\alpha = 0.05$), and Scheffe's multiple comparison test ($\alpha = 0.05$) were used for quantitative analysis of the data. The unbalanced one-way ANOVA was used to test for significant differences between the class means. If the differences were significant, then the multiple comparison tests were conducted to identify suitable bands for separating damaged saltcedar trees from other cover types.

3. Results

ANOVA results indicated significant differences ($\alpha = 0.05$) existed among class means for all of bands tested, resulting in further analysis of data with Scheffe's test. At site one on 24 August 2010, saltcedar trees exhibiting severe stress caused by beetle and larvae feeding were differentiated from other features with the red band (Table 2). Severely stressed saltcedar trees red reflectance were significantly higher than other vegetation types and blacktop-road and significantly lower ($\alpha = 0.05$) than soil and gravel (Table 2). Additionally, the near-infrared bands showed promise for discriminating severely stressed saltcedar trees from other vegetation, soil, and blacktop-road; however, those trees were not distinguishable from gravel. On 28 October 2010, none of the spectral bands differentiated stressed saltcedar trees from all of the other cover types (Table 3).

Site two results are summarised in Tables 4 and 5. Saltcedar canopies displaying stress symptoms initiated by beetle and larvae feeding were significantly different from other associated features for the coastal blue, blue, yellow, and red bands (Table 4) on 15 September 2010. Saltcedar canopies with greenish brown foliage (intermediate damage) were separated with the coastal blue, blue, and yellow bands; whereas, saltcedar trees with orange foliage (severe damage) were separable with the red band. Plants exhibiting these symptoms had significantly higher reflectance compared with other

Table 1. Number of spectral samples collected at each location per date.

Location	Date	Feature	Sample number
Site 1	24 August 2010	Saltcedar_SEV[a]	40
		Acacia spp.	41
		Cheeseweed	29
		Bermuda Grass	41
		Western Honey Mesquite	46
		Soil	41
		Gravel	41
		Blacktop-road	40
	28 October 2010	Saltcedar H	40
		Saltcedar_INT	44
		Saltcedar_SEV	24
		Acacia spp.	51
		Cheeseweed	20
		Bermuda Grass	35
		Western Honey Mesquite	39
		Soil	39
		Gravel	33
		Blacktop-road	33
Site 2	15 September 2010	Saltcedar H	46
		Saltcedar_INT	52
		Saltcedar_SEV	53
		Western Honey Mesquite	53
		Soil	43
		Blacktop-road	42
	21 July 2011	Saltcedar_DEF	33
		Western Honey Mesquite	50
		Soil	41
		Soil Plant Litter Mix	41
		Gravel	41
		Blacktop-road	42

[a]Saltcedar_INT = intermediate damage-mixture of green and brown foliage; Saltcedar_H = healthy-green foliage; Saltcedar_SEV = severe damage-mixture of green and brown foliage; Saltcedar_DEF = saltcedar defoliated.

plants. On 21 July 2011, the canopies of saltcedar trees were totally defoliated by the beetle and larvae. These trees were distinguishable from other land cover types with near-infrared bands (Table 5). Defoliated trees near-infrared reflectance was significantly lower ($\alpha = 0.05$) than all of the other cover types excluding blacktop-road in which reflectance was significantly higher.

4. Discussion

Saltcedar trees exhibiting damage from beetle and larvae feeding were commonly distinguished from other features with visible and near-infrared spectra. Separation was site, time, and cover type dependent (Tables 2–5). The red band was normally more consistent than other visible bands for discriminating changes in saltcedar foliage from other cover types. A healthy green plant leaf typically has low reflectance in the visible spectral region because of strong absorption by chlorophyll (Knipling 1970; Campbell 2002). Feeding damage affects the plant's ability to complete photosynthesis, causing chlorophyll to deteriorate and absorb less efficiently, thus increasing the visible reflectance.

Table 2. Matrix summarising the Scheffe's multiple range results of mean reflectance values for saltcedar trees exhibiting feeding damage from leaf beetles and for other features at study site one on 24 August 2010.

	Feature[b]	1	2	3	4	5	6	7	8
Coastal Blue[a] (400–450 nm)									
Mean ± STD									
0.0440 ± 0.013 (n = 40)[c]	1								
0.0223 ± 0.004 (n = 41)	2	**							
0.0453 ± 0.013 (n = 29)	3	NS	**						
0.0557 ± 0.008 (n = 41)	4	**	**	**					
0.0348 ± 0.010 (n = 46)	5	**	**	**	**				
0.1839 ± 0.005 (n = 41)	6	**	**	**	**	**			
0.1470 ± 0.013 (n = 41)	7	**	**	**	**	**	**		
0.0552 ± 0.002 (n = 40)	8	**	**	**	NS	**	**	**	
Blue (450–510 nm)									
Mean ± STD									
0.0549 ± 0.016 (n = 40)	1								
0.0325 ± 0.006 (n = 41)	2	**							
0.0609 ± 0.018 (n = 29)	3	NS	**						
0.0718 ± 0.011 (n = 41)	4	**	**	**					
0.0496 ± 0.011 (n = 46)	5	NS	**	**	**				
0.2165 ± 0.006 (n = 41)	6	**	**	**	**	**			
0.1638 ± 0.015 (n = 41)	7	**	**	**	**	**	**		
0.0593 ± 0.003 (n = 40)	8	NS	**	NS	**	**	**	**	
Green (510–580 nm)									
Mean ± STD									
0.0758 ± 0.019 (n = 40)	1								
0.0561 ± 0.011 (n = 41)	2	**							
0.0983 ± 0.029 (n = 29)	3	**	**						
0.1104 ± 0.012 (n = 41)	4	**	**	NS					
0.0852 ± 0.016 (n = 46)	5	NS	**	NS	**				
0.2594 ± 0.007 (n = 41)	6	**	**	**	**	**			
0.1884 ± 0.018 (n = 41)	7	**	**	**	**	**	**		
0.0561 ± 0.003 (n = 40)	8	NS	NS	NS	**	**	**	**	
Yellow (585–625 nm)									
Mean ± STD									
0.1030 ± 0.023 (n = 40)	1								
0.0510 ± 0.010 (n = 41)	2	**							
0.1012 ± 0.030 (n = 29)	3	NS	**						
0.1111 ± 0.017 (n = 41)	4	NS	**	NS					
0.0795 ± 0.019 (n = 46)	5	**	**	**	**				
0.3042 ± 0.007 (n = 41)	6	**	**	**	**	**			
0.2151 ± 0.021 (n = 41)	7	**	**	**	**	**	**		
0.0741 ± 0.003 (n = 40)	8	**	**	**	**	NS	**	**	
Red (630–690 nm)									
Mean ± STD									
0.1271 ± 0.028 (n = 40)	1								
0.0432 ± 0.009 (n = 41)	2	**							
0.0965 ± 0.030 (n = 29)	3	**	**						
0.1078 ± 0.020 (n = 41)	4	**	**	NS					
0.0678 ± 0.020 (n = 46)	5	**	**	**	**				

(*Continued*)

Table 2. (*Continued*)

	Feature	1	2	3	4	5	6	7	8
0.3269 ± 0.008 (n = 41)	6	**	**	**	**	**			
0.2258 ± 0.022 (n = 41)	7	**	**	**	**	**	**		
0.0787 ± 0.004 (n = 40)	8	**	**	**	**	NS	**	**	
Red edge (705–745 nm)									
Mean ± STD									
0.1686 ± 0.034 (n = 40)	1								
0.1653 ± 0.032 (n = 41)	2	NS							
0.2184 ± 0.061 (n = 29)	3	**	**						
0.2412 ± 0.016 (n = 41)	4	**	**	NS					
0.2394 ± 0.032 (n = 46)	5	**	**	NS	NS				
0.3519 ± 0.008 (n = 41)	6	**	**	**	**	**			
0.2360 ± 0.022 (n = 41)	7	**	**	NS	NS	NS	**		
0.0834 ± 0.004 (n = 40)	8	**	**	**	**	**	**	**	
Near-infrared 1 (770–895 nm)									
Mean ± STD									
0.2189 ± 0.044 (n = 40)	1								
0.2739 ± 0.056 (n = 41)	2	**							
0.2994 ± 0.079 (n = 29)	3	**	NS						
0.3583 ± 0.031 (n = 41)	4	**	**	**					
0.3649 ± 0.045 (n = 46)	5	**	**	**	NS				
0.3737 ± 0.008 (n = 41)	6	**	**	**	NS	NS			
0.2386 ± 0.023 (n = 41)	7	NS	**	**	**	**	**		
0.0892 ± 0.004 (n = 40)	8	**	**	**	**	**	**	**	
Near-infrared 2 (860–1040 nm)									
Mean ± STD									
0.2454 ± 0.049 (n = 40)	1								
0.2819 ± 0.056 (n = 41)	2	**							
0.3165 ± 0.083 (n = 29)	3	**	NS						
0.3710 ± 0.030 (n = 41)	4	**	**	**					
0.3709 ± 0.046 (n = 46)	5	**	**	**	NS				
0.3840 ± 0.008 (n = 41)	6	**	**	**	NS	NS			
0.2379 ± 0.023 (n = 41)	7	NS	**	**	**	**	**		
0.0943 ± 0.004 (n = 40)	8	**	**	**	**	**	**	**	

[a]Data were averaged to simulate WorldView2 spectra.
[b]Feature: 1 = saltcedar severe damage-mixture of green and brown foliage, 2 = *Acacia* spp., 3 = cheeseweed, 4 = Bermuda grass, 5 = western honey mesquite, 6 = soil, 7 = gravel, and 8 = blacktop-road.
[c]**Significantly different $\alpha = 0.05$, NS = not significant;
**NS only applies to mean reflectance for a specific wavelength and are not to be compared across wavelengths.

As expected, both near-infrared bands were useful for distinguishing defoliated saltcedar trees. The green band also showed promise for separating defoliated trees from other features. Healthy green vegetation highly reflects near-infrared light and moderately reflects green light (Knipling 1970; Campbell 2002). Absence of foliage caused differences observed between defoliated saltcedar trees and other land cover types (Knipling 1970). Beetle and larvae feeding on saltcedar leaves affects foliar constituents and foliage amount, thus influencing the reflectance of light energy, thereby altering the reflectance spectrum of the tree. Other researchers have used this concept as the basis for detecting insect damage to plant leaves and canopies (Ahern 1988; Vogelman et al. 1993; Cook et al. 2010). Furthermore after defoliation of the trees, soil, grass, and plant

Table 3. Matrix summarising the Scheffe's multiple range results of mean reflectance values for saltcedar trees exhibiting feeding damage from leaf beetles and for other features at study site one on 28 October 2010.

	Feature[b]	1	2	3	4	5	6	7	8	9	10
Coastal Blue[a] (400–450 nm)											
Mean ± STD											
0.0520 ± 0.013 (n = 40)[c]	1										
0.0700 ± 0.010 (n = 44)	2	**									
0.0511 ± 0.016 (n = 24)	3	NS	**								
0.0225 ± 0.005 (n = 51)	4	**	**	**							
0.0502 ± 0.016 (n = 20)	5	NS	**	NS	**						
0.0649 ± 0.007 (n = 35)	6	**	NS	**	**	**					
0.0532 ± 0.014 (n = 39)	7	NS	**	NS	**	NS	**				
0.1814 ± 0.011 (n = 39)	8	**	**	**	**	**	**	**			
0.1209 ± 0.006 (n = 33)	9	**	**	**	**	**	**	**	**		
0.0544 ± 0.002 (n = 33)	10	NS	**	NS	**	NS	NS	NS	**	**	
Blue (450–510 nm)											
Mean ± STD											
0.0613 ± 0.017(n = 40)	1										
0.0948 ± 0.013 (n = 44)	2	**									
0.0665 ± 0.021 (n = 24)	3	NS	**								
0.0344 ± 0.008 (n = 51)	4	**	**	**							
0.0745 ± 0.027 (n = 20)	5	NS	**	NS	**						
0.0891 ± 0.009 (n = 35)	6	NS	NS	**	**	NS					
0.0788 ± 0.021 (n = 39)	7	**	**	NS	**	NS	NS				
0.2166 0.012 (n = 39)	8	**	**	**	**	**	**	**			
0.1334 ± 0.007 (n = 33)	9	**	**	**	**	**	**	**	**		
0.0581 ± 0.002 (n = 33)	10	NS	**	**	**	**	**	**	**	**	
Green (510–580 nm)											
Mean ± STD											
0.1006 ± 0.024 (n = 40)	1										
0.1379 ± 0.017 (n = 44)	2	**									
0.0936 ± 0.029 (n = 24)	3	NS	**								
0.0643 ± 0.015 (n = 51)	4	**	**	**							
0.1221 ± 0.039 (n = 20)	5	NS	NS	**	**						
0.1348 ± 0.011 (n = 35)	6	**	NS	**	**	NS					
0.1283 ± 0.032 (n = 39)	7	**	NS	**	**	NS	NS				
0.2654 ± 0.015 (n = 39)	8	**	**	**	**	**	**	**			
0.1527 ± 0.009 (n = 33)	9	**	NS	**	**	**	NS	**	**		
0.0593 ± 0.064 (n = 33)	10	**	**	**	NS	**	**	**	**	**	
Yellow (585–625 nm)											
Mean ± STD											
0.0907 ± 0.027 (n = 40)	1										
0.1507 ± 0.022 (n = 44)	2	**									
0.1229 ± 0.033 (n = 24)	3	**	**								
0.0541 ± 0.014 (n = 51)	4	**	**	**							
0.1292 ± 0.045 (n = 20)	5	**	NS	NS	**						
0.1468 ± 0.014 (n = 35)	6	**	NS	NS	**	NS					
0.1343 ± 0.039 (n = 39)	7	**	NS	NS	**	NS	NS				
0.3475 ± 0.017 (n = 39)	8	**	**	**	**	**	**	**			
0.1748 ± 0.010 (n = 33)	9	**	**	**	**	**	**	**	**		
0.0720 ± 0.002 (n = 33)	10	NS	NS	**	NS	**	**	**	**	**	

(*Continued*)

Table 3. (*Continued*)

	Feature	1	2	3	4	5	6	7	8	9	10
Red (630–690 nm)											
Mean ± STD											
0.0807 ± 0.029 (n = 40)	1										
0.1502 ± 0.023 (n = 44)	2	**									
0.1393 ± 0.035 (n = 24)	3	**	NS								
0.0447 ± 0.012 (n = 51)	4	**	**	**							
0.1267 ± 0.049 (n = 20)	5	**	NS	NS	**						
0.1489 ± 0.017 (n = 35)	6	**	NS	NS	**	NS					
0.1261 ± 0.043 (n = 39)	7	**	NS	NS	**	NS	NS				
0.3475 ± 0.017 (n = 39)	8	**	**	**	**	**	**	**			
0.1843 ± 0.011(n = 33)	9	**	**	**	**	**	**	**	**		
0.0764 ± 0.003(n = 33)	10	NS	**	**	**	**	**	**	**	**	
Red edge (705–745 nm)											
Mean ± STD											
0.2970 ± 0.057 (n = 40)	1										
0.2900 ± 0.034 (n = 44)	2	NS									
0.2138 ± 0.054 (n = 24)	3	**	**								
0.1913 ± 0.049 (n = 51)	4	**	**	NS							
0.2915 ± 0.077 (n = 20)	5	NS	NS	**	**						
0.2922 ± 0.017 (n = 35)	6	NS	NS	**	**	NS					
0.3334 ± 0.068 (n = 39)	7	NS	**	**	**	NS	NS				
0.3723 ± 0.018 (n = 39)	8	**	**	**	**	**	**	NS			
0.1959 ± 0.012 (n = 33)	9	**	**	NS	NS	**	**	**	**		
0.0861 ± 0.003 (n = 33)	10	**	**	**	**	**	**	**	**	**	
Near-infrared 1 (770–895 nm)											
Mean ± STD											
0.4693 ± 0.085 (n = 40)	1										
0.3837 ± 0.044 (n = 44)	2	**									
0.2804 ± 0.068 (n = 24)	3	**	**								
0.3389 ± 0.087 (n = 51)	4	**	NS	NS							
0.4139 ± 0.102 (n = 20)	5	NS	NS	**	**						
0.4102 ± 0.034 (n = 35)	6	NS	NS	**	**	NS					
0.4768 ± 0.094 (n = 39)	7	NS	**	**	**	NS	**				
0.3962 ± 0.018 (n = 39)	8	**	NS	**	NS	NS	NS	**			
0.2002 ± 0.012 (n = 33)	9	**	**	**	**	**	**	**	**		
0.0871 ± 0.003 (n = 33)	10	**	**	**	**	**	**	**	**	**	
Near-infrared 2 (860–1040 nm)											
Mean ± STD											
0.4789 ± 0.084 (n = 40)	1										
0.4059 ± 0.046 (n = 44)	2	**									
0.3040 ± 0.072 (n = 24)	3	**	**								
0.3506 ± 0.089 (n = 41)	4	**	NS	NS							
0.4372 ± 0.109 (n = 51)	5	NS	NS	**	**						
0.4368 ± 0.033 (n = 20)	6	NS	NS	**	**	NS					
0.4921 ± 0.097 (n = 35)	7	NS	**	**	**	NS	NS				
0.4099 ± 0.019 (n = 39)	8	**	NS	**	**	NS	NS	**			
0.2009 ± 0.013(n = 39)	9	**	**	**	**	**	**	**	**		
0.0918 ± 0.003 (n = 33)	10	**	**	**	**	**	**	**	**	**	

[a]Data were averaged to simulate WorldView2 spectra.
[b]Feature: 1 = saltcedar healthy green foliage, 2 = saltcedar intermediate damage-mixture of green and brown foliage, 3 = saltcedar severe damage-orange foliage, 4 = *Acacia* spp., 5 = cheeseweed, 6 = Bermuda grass, 7 = western honey mesquite, 8 = soil, 9 = gravel, and 10 = blacktop-road.
[c]**Significantly different $\alpha = 0.05$, NS = not significant;
**NS only applies to mean reflectance for a specific wavelength and are not to be compared across wavelengths.

Table 4. Matrix summarising the Scheffe's multiple range results for mean reflectance values of saltcedar trees exhibiting feeding damage from leaf beetles and for other features at study site two on 15 September 2010.

	Feature[b]	1	2	3	4	5	6
Coastal Blue[a] (400–450 nm)							
Mean ± STD							
0.0390 ± 0.007 (n = 46)[c]	1						
0.0457 ± 0.008 (n = 52)	2	**					
0.0361 ± 0.006 (n = 53)	3	NS	**				
0.0390 ± 0.012 (n = 53)	4	NS	**	NS			
0.0644 ± 0.003 (n = 43)	5	**	**	**	**		
0.0744 ± 0.003 (n = 42)	6	**	**	**	**	**	
Blue (450–510 nm)							
Mean ± STD							
0.0480 ± 0.080 (n = 46)	1						
0.0689 ± 0.013 (n = 52)	2	**					
0.0574 ± 0.010 (n = 53)	3	**	**				
0.0531 ± 0.015 (n = 53)	4	NS	**	NS			
0.0798 ± 0.043 (n = 43)	5	**	**	**	**		
0.0836 ± 0.003 (n = 42)	6	**	**	**	**	NS	
Green (510–580 nm)							
Mean ± STD							
0.0763 ± 0.012 (n = 46)	1						
0.0940 ± 0.019 (n = 52)	2	**					
0.0895 ± 0.016 (n = 53)	3	**	NS				
0.0818 ± 0.022 (n = 53)	4	NS	**	NS			
0.1080 ± 0.006 (n = 43)	5	**	**	**	**		
0.0977 ± 0.004 (n = 42)	6	**	NS	**	**	NS	
Yellow (585–625 nm)							
Mean ± STD							
0.0688 ± 0.012 (n = 46)	1						
0.1160 ± 0.024 (n = 52)	2	**					
0.1333 ± 0.025 (n = 53)	3	**	**				
0.0817 ± 0.024 (n = 53)	4	NS	**	**			
0.1428 ± 0.008 (n = 43)	5	**	**	NS	**		
0.1749 ± 0.037 (n = 42)	6	**	**	**	**	**	
Red (630–690 nm)							
Mean ± STD							
0.0587 ± 0.011 (n = 46)	1						
0.1259 ± 0.028 (n = 52)	2	**					
0.1759 ± 0.034 (n = 53)	3	**	**				
0.0754 ± 0.025 (n = 53)	4	**	**	**			
0.1592 ± 0.009 (n = 43)	5	**	**	**	**		
0.1215 ± 0.005 (n = 42)	6	**	NS	**	**	**	
Red edge (704–745 nm)							
Mean ± STD							
0.2201 ± 0.035 (n = 46)	1						
0.2026 ± 0.039 (n = 52)	2	NS					
0.2436 ± 0.046 (n = 53)	3	NS	**				
0.2016 ± 0.044 (n = 53)	4	NS	NS	**			

(*Continued*)

Table 4. (*Continued*).

	Feature[b]	1	2	3	4	5	6
0.1776 ± 0.011 (n = 43)	5	**	**	**	NS		
0.1296 ± 0.006 (n = 42)	6	**	**	**	**	**	
Near-infrared 1 (770–895 nm)							
Mean ± STD							
0.3544 ± 0.057 (n = 46)	1						
0.2760 ± 0.050 (n = 52)	2	**					
0.3223 ± 0.060 (n = 53)	3	NS	**				
0.3037 ± 0.060 (n = 53)	4	**	NS	NS			
0.1915 ± 0.014 (n = 43)	5	**	**	**	**		
0.1368 ± 0.006 (n = 42)	6	**	**	**	**	**	
Near-infrared 2 (860–1040 nm)							
Mean ± STD							
0.3656 ± 0.057 (n = 46)	1						
0.3099 ± 0.057 (n = 52)	2	**					
0.3590 ± 0.066 (n = 53)	3	NS	**				
0.3131 ± 0.061 (n = 53)	4	**	NS	**			
0.1958 ± 0.016 (n = 43)	5	**	**	**	**		
0.1415 ± 0.006 (n = 42)	6	**	**	**	**	**	

[a]Data were averaged to simulate WorldView2 spectra.
[b]Feature: 1 = saltcedar healthy green foliage, 2 = saltcedar intermediate damage-mixture of green and brown foliage, 3 = saltcedar severe damage-orange foliage, 4 = western honey mesquite, 5 = soil, and 6 = blacktop-road.
[c]**Significantly different $\alpha = 0.05$, NS = not significant;
**NS only applies to mean reflectance for a specific wavelength and are not to be compared across wavelengths.

litter previously obscured by tree foliage were partially visible through openings between the branches. Therefore, these materials also contributed to spectral responses of defoliated trees and differences observed between defoliated trees and other cover types.

Everitt et al. (2007) separated healthy saltcedar plants from saltcedar plants exhibiting stress caused by the saltcedar leaf beetle. Their study only focused on saltcedar trees. The current study compared the stress levels to associated land cover types. Additionally, Everitt et al. (2007) evaluated 10 nm spectral bands centred at blue (450 nm), green (550 nm), and red (675 nm) wavelengths. Findings of the current study suggested that spectral bands with broader wavelengths can distinguish beetle and larvae feeding related stress to saltcedar trees from other features.

It was not exactly known why the stressed saltcedar trees could not be distinguished from other vegetation types at site one on 28 October 2010. Cheeseweed canopies contained blooms, leaf dieback was noticed in western honey mesquite, and bermuda grass appeared in mixtures of green and brown colours. It is speculated that changes observed in these plant canopies contributed to the non-significant differences observed between stressed saltcedar trees and other vegetation.

To put this study into perspective, ground-based field data were evaluated to compare and contrast the spectra of saltcedar tree canopies affected by the biological control agent saltcedar leaf beetle with other associated cover types. From an airborne and

Table 5. Matrix summarising the Scheffe's multiple range results of mean reflectance values for saltcedar trees exhibiting feeding damage from leaf beetles and for other features at study site two on 21 July 2011.

	Feature	1	2	3	4	5	6
Coastal Blue[a] (400–450 nm)							
Mean ± STD							
0.0400 ± 0.013 (n = 33)[c]	1						
0.0384 ± 0.010 (n = 50)	2	NS					
0.1254 ± 0.006 (n = 41)	3	**	**				
0.0763 ± 0.004 (n = 41)	4	**	**	**			
0.1280 ± 0.005 (n = 41)	5	**	**	NS	**		
0.0654 ± 0.006 (n = 42)	6	**	**	**	**	**	
Blue (450–510 nm)							
Mean ± STD							
0.0494d ± 0.016 (n = 33)	1						
0.0524d ± 0.013 (n = 50)	2	NS					
0.1504a ± 0.007 (n = 41)	3	**	**				
0.0990b ± 0.005 (n = 41)	4	**	**	**			
0.1476a ± 0.005 (n = 41)	5	**	**	NS	**		
0.0730c ± 0.007 (n = 42)	6	**	**	**	**	**	
Green (510–580 nm)							
Mean ± STD							
0.0639 ± 0.020 (n = 33)	1						
0.0847 ± 0.019 (n = 50)	2	**					
0.1910 ± 0.009 (n = 41)	3	**	**				
0.1306 ± 0.007 (n = 41)	4	**	**	**			
0.1793 ± 0.006 (n = 41)	5	**	**	**	**		
0.0850 ± 0.009 (n = 42)	6	**	NS	**	**	**	
Yellow (585–625 nm)							
Mean ± STD							
0.0827 ± 0.026 (n = 33)	1						
0.0789 ± 0.022 (n = 50)	2	NS					
0.2377 ± 0.011 (n = 41)	3	**	**				
0.1647 ± 0.009 (n = 41)	4	**	**	**			
0.2166 ± 0.007 (n = 41)	5	**	**	**	**		
0.0982 ± 0.012 (n = 42)	6	**	**	**	**	**	
Red (630–690 nm)							
Mean ± STD							
0.1015 ± 0.029 (n = 33)	1						
0.0696 ± 0.025 (n = 50)	2	**					
0.2589 ± 0.012 (n = 41)	3	**	**				
0.1946 ± 0.011 (n = 41)	4	**	**	**			
0.2331 ± 0.007 (n = 41)	5	**	**	**	**		
0.1046d ± 0.012 (n = 42)	6	NS	**	**	**	**	
Red edge (705–745 nm)							
Mean ± STD							
0.1268 ± 0.034 (n = 33)	1						
0.2347 ± 0.039 (n = 50)	2	**					
0.2769 ± 0.013 (n = 41)	3	**	**				

(*Continued*)

Table 5. (*Continued*).

	Feature	1	2	3	4	5	6
0.2322 ± 1.012 (n = 41)	4	**	NS	**			
0.2472 ± 0.008 (n = 41)	5	**	NS	**	NS		
0.1109 ± 0.013 (n = 42)	6	NS	**	**	**	**	
Near-infrared 1 (770–895 nm)							
Mean ± STD							
0.1642d ± 0.042 (n = 33)	1						
0.3728a ± 0.059 (n = 50)	2	**					
0.2918b ± 0.013 (n = 41)	3	**	**				
0.2906b ± 0.014 (n = 41)	4	**	**	NS			
0.2548c ± 0.010 (n = 41)	5	**	**	**	**		
0.1161e ± 0.014 (n = 42)	6	**	**	**	**	**	
Near-infrared 2 (860–1040 nm)							
Mean ± STD							
0.1907 ± 0.047 (n = 33)	1						
0.3776 ± 0.058 (n = 50)	2	**					
0.2964 ± 0.013 (n = 41)	3	**	**				
0.3377 ± 0.018 (n = 41)	4	**	**	**			
0.2549 ± 0.012 (n = 41)	5	**	**	**	**		
0.1187 ± 0.014 (n = 42)	6	**	**	**	**	**	

[a]Data were averaged to simulate WorldView2 spectra.
[b]Feature: 1 = saltcedar defoliated, 2 = western honey mesquite, 3 = soil, 4 = soil plant litter mix, 5 = gravel, and 6 = blacktop-road.
[c]**Significantly different $\alpha = 0.05$, NS = not significant;
**NS only applies to mean reflectance for a specific wavelength and are not to be compared across wavelengths.

satellite sensor viewpoint, tree-crown density, leaf shape and orientation, background canopy reflectance, measurement geometry, and in-canopy shadowing will have more of an influence on the digital count and/or reflectance value recorded in a pixel (Asner 1998). Additionally for severely damaged and defoliated trees, the pixel value will be an integration of defoliated branches and soil, vegetation, and plant litter found underneath the tree. It is believed that background material will have more of an effect in areas where trees are not densely clustered. Furthermore, simulated measurements do not account for atmospheric effects; nevertheless, the simulated data do provide information related to the potential of spectral bands to separate the individual components. Therefore, it is believed airborne and satellite-borne broadband multispectral sensors are applicable as tools to monitor biological control of saltcedar.

Single bands were evaluated in this study. Dennison et al. (2009) have shown the potential of vegetation indices to monitor defoliation of trees by the beetle. With the overabundance of vegetation indices available, future research should determine the potential of using vegetation indices to separate saltcedar trees exhibiting multiple feeding damage levels from other vegetation types and human made features.

5. Summary

This study was conducted to evaluate broadband spectra within visible, red-edge, and near-infrared wavelengths to discriminate saltcedar trees exhibiting feeding damage caused by the saltcedar leaf beetle from other land cover types. Visible bands were important for distinguishing feeding stress saltcedar trees from other cover types;

near-infrared and green spectra were useful for discriminating totally defoliated saltcedar trees. Findings of this study further encourage exploration of airborne and satellite borne data for monitoring biological control of saltcedar in west Texas and other areas throughout the US.

Acknowledgements

The author is grateful to Juan Ramos, Isabel Cavazos, Dr Chris Ritzi, Dr Jack DeLoach, Dr Patrick Moran, James Tracey, Anne Hilscher, and Pat Sims for their assistance in this study.

References

Ahern FJ. 1988. The effects of bark beetle stress on the foliar spectral reflectance of lodgepole pine. Int J Rem Sens. 9:1451–1468.

Anderson GL, Carruthers RI, Shaokui G, Gong P. 2005. Monitoring of invasive Tamarix distribution and effects of biological control with airborne hyperspectral remote sensing. Int J Rem Sens. 26:2487–2489.

Asner GP. 1998. Biophysical and biochemical sources of variability in canopy reflectance. Remote Sens Environ. 64:234–253.

Bailey JK, Scheitzer JA, Whitham TG. 2001. Salt cedar negatively affects biodiversity of aquatic macroinvertebrates. Wetlands. 21:442–447.

BASF. 2005. Saltcedar: plant with unquenchable thirst threatens habitats, water supplies [Internet]. Available from: http://www.vmanswers.com/reference/literature/saltcedar-technical-bulletin-.pdf

Blackburn W, Knight RW, Schuster JL. 1982. Saltcedar influence on sedimentation in the Brazos River. J Soil Water Conser. 37:298–301.

Brotherson JD, Field D. 1987. *Tamarix*: impacts of a successful weed. Rangelands. 9:110–112.

Campbell JB. 2002. Introduction to remote sensing. New York (NY): The Guilford Press.

Cook S, Humes K, Hruska R, Williams C, Fraley G. 2010. Previsual detection of two conifer-infesting adelgid species in North American forests. In: Pye JM, Rauscher HM, Sands Y, Lee DC, Beatty JS, editors. Advances in threat assessment and their application to forest and rangeland management. USDA Forest Service. General Technical Report PNW-GTR 802. p. 551–558.

DeLoach CJ. 1991. Saltcedar, an exotic weed of Western North American Riparian areas: a review of its taxonomy, biology, harmful and beneficial values, and its potential for biological control. USDI Bureau of Reclamation, Lower Colorado Region, Final Report. Boulder City, Nevada, 433 p.

DeLoach CJ, Carruthers RI. 2004. Biological control programs for integrated invasive weed management. In: Proceedings of Weed Science Society of America Meeting, Kansas City, MO. Weed Science Society of America (CD-ROM), 17 pp.

DeLoach CJ, Carruthers RI, Lovich JE, Dudley TL, Smith SD. 2000. Ecological interactions in the biological control of saltcedar (*Tamarix* spp.) in the United States: toward a new understanding. In: Spencer NR, editor. Proceedings of the X International Symposium on Biological Control of Weeds; 1999 Jul 4–14; Bozeman, MT: Montana University, 819–873.

DeLoach CJ, Lewis PA, Herr JC, Carruthers RI, Tracy JL, Johnson J. 2003. Host specificity of the leaf beetle, *Diorhabda elongate deserticola* (Coleoptera: Chrysomelidae) from Asia, a biological control agent saltcedars (*Tamarix*: Tamaricaceae) in the Western United States. Biol Control. 27:117–147.

DeLoach CJ, Milbrath LR, Carruthers R, Knutson AE, Nibling F, Eberts D, Thompson DC, Kazmer DJ, Dudley T, Bean DW, Knight JB. 2006. Overview of saltcedar biological control. In: USDA Forest Service Proceedings, Fort Collins, CO: U.S. Department of Agriculture, Forest Service, Rocky Mountain Research Station. RMRS-P-42CD.

Dennison PE, Nagler PL, Hultine KR, Glenn EP, Ehleringer JR. 2009. Remote monitoring of tamarisk defoliation and evapotranspiration following saltcedar leaf beetle attack. Remote Sens Environ. 113:1462–1472.

DiTomaso JM. 1998. Impact, biology, and ecology of saltcedar (*Tamarix* spp.) in the southwestern United States. Weed Technol. 12:326–336.

Dudley TL, DeLoach CJ, Lovich JE, Carruthers RI. 2000. Saltcedar invasion of western riparian areas: impacts and new prospects for control. Trans North Am Wildlife Nat Resour Conf. 65:345–381.

Everitt JH, Yang C, Fletcher RS, DeLoach CJ, Davis MR. 2007. Using remote sensing to assess biological control of saltcedar. Southwest Entomol. 32:93–103.

Gaskin JF, Schaal BA. 2003. Molecular phylogenetic investigation of US invasive *Tamarix*. Syst Bot. 28:86–95.

Knipling EB. 1970. Physical and physiological basis for the reflectance of visible and near-infrared radiation from vegetation. Remote Sens Environ. 54:155–159.

Knutson A, Muegge M, DeLoach J. 2009. Biological control of Tamarix in Texas. Western Society of Weed Science Symposium [Internet]. Available from: http://www.wsweed science.org/Slides/2009/Biocontrol%20Symposium/10%20Biological%20Control%20of%20Tamarix%20in%20Texas%20-%20Knutson.pdf

Knutson A, Muegge M, DeLoach J. 2011. Biological control of saltcedar. Texas A&M AgriLife Extension Service, Bulletin, L-5444, 1–6.

Lewis PA, DeLoach CJ, Knutson AE, Tracy JL, Robbins TO. 2003. Biology of *Oiorhabda elongata deserticola* (Coleoptera: Chrysomelidae), an Asian leaf beetle for biological control of saltcedar (*Tamarix* spp.) in the United States. Biol Control. 27:101–116.

Lovich JE, DeGouvenain RC. 1998. Saltcedar invasion in desert wetlands of the southwestern United States: ecological and political implications. In: Majumdar SK, Miller EW, Brenner FJ, editors. Ecology of wetlands and associated systems. Easton (PA): Pennsylvania Academy of Science, 447–467.

Lovich JE, Egan TB, DeGouvenain RC. 1994. Tamarisk control on public lands in the desert of southern California: two case studies. In: Proceedings of the 46th Annual California Weeds Conference, 1993; Fremont, CA: California Weed Science Society, 166–177.

Ritzi CM, Hilscher AM. 2010. Saltcedar beetle project [Internet]. Available from: http://www.sulross.edu/scbp

Ritzi CM, Hilscher AM. 2011. Saltcedar beetle project [Internet]. Available from: http://www.sulross.edu/scbp

Tracy JL, DeLoach CJ. 1999. Biological control of saltcedar in the United States: progress and projected ecological effects. In: Bell CE, editor. Proceedings of the Arundo and Saltcedar Workshop; 1998 June 17; Ontario, CA, 111–154.

Trigg S, Flasse S. 2000. Characterizing the spectral-temporal response of burned savannah using *in situ* spectroradiometry and infrared thermometry. Int J Rem Sens. 21:3161–3168.

US Fish and Wildlife Service. 1998. Endangered and threatened wildlife and plants: proposed threatened status for the plant "Helianthus paradoxus" (Pecos sunflower). Fed Reg. 63:15808–15813.

USDA. 2005. Program for biological control of saltcedar (*Tamarix* spp.) in thirteen states. Fort Collins, Colorado (USA): United States Department of Agriculture – Animal and Plant Health Inspection Service.

Vogelman JE, Rock BN, Moss DM. 1993. Red edge spectral measurements from sugar maple leaves. Int J Rem Sens. 14:1563–1575.

Zouhar K. 2003. *Tamarix* spp. in: fire effects information system [Internet]. US Department of Agriculture, Forest Service, Rocky Mountain Research Station, Fire Sciences Laboratory (Producer). Available from: http://www.fs.fed.us/database/feis/plants/tree/tamspp/all.html